Theoretical Notes
Note 362

10 June 1991

Diffraction Past a Perfectly Conducting Sphere Embedded in a Conductor

Clifford W. Prettie
Berkeley Research Associates, P. O. Box 241, Berkeley, CA 94701

Abstract

The Mie series for the field scattered by a perfectly conducting sphere has been evaluated and plotted for complex values of wavenumber in order to explore the near-field shadowing properties of objects in a lossy dielectric or in a conducting medium. The existence of near field shadows appears to be controlled by the product of the magnitude of the wavenumber and the structure size. The shadows produced in a lossy dielectric were spatially smoother than those produced in dielectric with the same magnitude wavenumber. For conducting media with skin depths smaller than the radius of the sphere by a factor of three or more, shadows were produced.

Introduction

The diffraction of electromagnetic waves past various obstacles has been intensely studied over the last century. Many trends can be observed from the results of these analyses that provide a working understanding of the process. One of these trends relates to the shadowing properties of conducting objects. The issue of whether an object in vacuum produces a shadow or not depends upon its size with respect to a wavelength. Larger objects produce shadows whereas smaller objects do not. This trend is immediately transferable to the situation of an object embedded in an ideal dielectric. The shadowing property of the diffraction process is independent of the absolute speed of light; in a pure dielectric only the relation between wavelength and the object size is important.

At this point, the question that is the central concern of this short paper arises, namely, what are the shadowing properties of perfectly conducting objects embedded in media that are not pure dielectrics? In several geophysical and biosensing situations, diffraction phenomena must be considered for objects embedded in conducting media and their shadowing properties are important to understand. In a lossy medium the field decays exponentially with penetration depth. The concern of the paper has been losses over and above this baseline decay rate caused by the presence of conducting objects embedded within it.

As an initial consideration of this question, it can be noted that a conducting medium is mathematically equivalent to a medium with a complex dielectric constant. In the limit of a good conductor the dielectric constant has a value that is essentially pure imaginary. If an *a priori* attempt is made to anticipate the shadowing behavior based upon the value of the dielectric constant, the question of what parameter is most relevant arises. There are at least three obvious choices and two would suggest different results from the third for the case of a medium that is a good conductor.

For a fixed object size one conjecture is that the shadowing properties are dependent upon the magnitude of the complex wavenumber. One might arrive at this

guess based upon dimensional arguments alone. Another conjecture is that the shadowing properties are dependent upon the value of the real part of the wavenumber. This dependence might be anticipated if it were the case that shadowing is an interference phenomenon and that the interference between waves is dependent upon wave phase shift as controlled by the real part of the wavenumber. A third conjecture is that the real part of the dielectric constant (assumed to be essentially zero for a good conductor) is the important parameter for controlling shadowing because this value controls the magnitude of the component of the current that is in phase-quadrature with the electric field. If this were the case then the important parameter is the real part of the wavenumber squared. For the case of the lossless dielectric all three conjectures are consistent with known results. However, in lossy dielectrics there is a difference that becomes pronounced in the case where the dielectric is essentially a good conductor. The former two conjectures both suggest the result that objects larger than a skin depth produce shadows whereas the latter suggests that ratio with the skin depth is largely unimportant and that shadowing might not occur in good conductors with negligible dielectric constants.

Armed with these considerations the results from classical analyses are considered to address the shadowing issue. In particular the diffractive properties of a sphere are addressed. The sphere is chosen because its scattering behavior has been extensively studied. While asymptotic formulations such as GTD are applicable to the shadowing issue we have chosen not to deal with applying these techniques for complex wavenumbers and instead have opted for a numerical field calculation using the 'exact' Mie series. The availability of functions that are readily accessible for numerical computation of the scattered field is, thus, another motivating factor for the choice of a sphere.

Formulation -- Mie Series Approach

Much work has been performed in the past by others on the diffractive properties of the perfectly conducting sphere. The diffraction of a harmonic plane wave by a sphere is treated in various textbooks including Stratton (1941), King and Wu, (1959), Harrington, (1961), Jackson (1961), Panofsky and Phillips (1962), Jones (1964), Van Bladel, (1964) and Bowman, et al., (1969). In the series of interaction notes, Baum (1971), presents an excellent discussion of the singularity expansion method to the sphere problem. While the treatment is universally discussed in terms of real-valued wavenumbers, it is also applicable for complex values of k and is, thus, pertinent to the diffraction problem in a conducting medium. Following Harrington (1961) the scattered field for a sphere of radius 'a' can be written in terms of the potentials, A_r^s and F_r^s as:

$$A_r^s = \frac{E_0}{\omega\mu} \cos\phi \sum_{n=1}^{\infty} b_n \hat{H}_n^{(2)}(kr)\, P_n^1(\cos\theta)$$

$$F_r^s = \frac{E_0}{k} \sin\phi \sum_{n=1}^{\infty} c_n \hat{H}_n^{(2)}(kr)\, P_n^1(\cos\theta)$$

where $$b_n = -a_n \frac{\hat{J}_n'(ka)}{\hat{H}_n^{(2)\prime}(ka)}$$

$$c_n = -a_n \frac{\hat{J}_n(ka)}{\hat{H}_n^{(2)}(ka)}$$

and $$a_n = \frac{i^{-n}(2n+1)}{n(n+1)}$$

In these relations, A_r^s and F_r^s are the scattered radial components of the TM to r and TE to r field potentials. The scattered electric, $\mathbf{E}^s$, and magnetic, $\mathbf{H}^s$, field components may

be expressed in terms of these potentials as

$$E_r^s = \frac{1}{\hat{y}}\left[\frac{\partial^2}{\partial r^2} + k^2\right] A_r^s$$

$$E_\phi^s = \frac{-1}{r\sin\theta}\frac{\partial F_r^s}{\partial \phi} + \frac{1}{\hat{y}\, r}\frac{\partial^2 A_r^s}{\partial r\, \partial \theta}$$

$$E_\phi^s = \frac{1}{r}\frac{\partial F_r^s}{\partial \theta} + \frac{1}{\hat{y}\, r\sin\theta}\frac{\partial^2 A_r^s}{\partial r\, \partial \phi}$$

$$H_r^s = \frac{1}{\hat{z}}\left[\frac{\partial^2}{\partial r^2} + k^2\right] F_r^s$$

$$H_\theta^s = \frac{1}{r\sin\theta}\frac{\partial A_r^s}{\partial \phi} + \frac{1}{\hat{z}\, r}\frac{\partial^2 F_r^s}{\partial r\, \partial \theta}$$

$$H_\phi^s = -\frac{1}{r}\frac{\partial A_r^s}{\partial \theta} + \frac{1}{\hat{z}\, r\sin\theta}\frac{\partial^2 F_r^s}{\partial r \partial \phi}$$

As suggested by the variables standard spherical coordinates, r,θ,ϕ, are assumed. The incident plane wave approaches the sphere from the $-z$ axis ($\theta = 180°$). It has an electric field with magnitude E_0 pointed in the x-direction ($\mathbf{i}_x$). Its spatial dependence is

$$\mathbf{E}^{inc} = E_0 e^{-ikz}\ \mathbf{i}_x \quad .$$

where a harmonic time dependence of $e^{i\omega t}$ has been assumed. The radian frequency ω, is assumed to be real. The wavenumber, k, is complex if the medium is conductive. The value of k is given, in Harrington's (1961) notation, through the relation

$$k^2 = -\hat{z}\,\hat{y}$$

The value of $\hat{z}$ is defined by $\hat{z} = i\omega\mu$ where μ is the magnetic permeability of the medium. The permeability, μ, can be assumed to be that of vacuum ($4\pi \times 10^{-7}$ Henrys per meter) for the sake of this paper. The value of $\hat{y}$ is defined as $\hat{y} = i\omega\varepsilon + \sigma$ where ε is

the permittivity of the medium (in farads per meter) and where σ is the conductivity of the medium in Siemens (mhos per meter). For a medium that is primarily conductive, i.e., $\sigma \gg \omega\varepsilon$, the value of k is

$$k = (1-i)/\delta$$

where δ is the skin depth $\delta = \left[\frac{2}{\omega\mu\sigma}\right]^{1/2}$. An upward going wave involves the factor

$$e^{-ikz} = e^{-iz/\delta}\, e^{-z/\delta}$$

It decays one e-fold in magnitude and shifts phase one radian for every skin depth propagated.

The radial dependence of the scattered potentials and scattering coefficients are expressed in terms of the spherical Bessel functions of Schelkunoff, frequently called Ricatti-Bessel functions, and are denoted with a hat to indicate their association with standard Bessel functions, i.e.,:

$$\hat{B}_n(z) \equiv \left[\frac{\pi z}{2}\right]^{1/2} B_{n+1/2}(z)$$

where B_n stands for J_n, Y_n or H_n denoting Bessel, Neumann or Hankel functions. In the terms $\hat{H}_n^{(2)}(z)$ the superscript '(2)' denotes the Hankel function of the second kind, i.e., $\hat{H}_n^{(2)} = \hat{J}_n - i\hat{Y}_n$. Primes next to these functions denote first derivatives. The expressions for the scattered potential also involve the Legendre functions of degree n and order 1, P_n^1.

To address the issue of shadowing for a sphere embedded in a conductor the series for the scattered field has been evaluated and used to determine the total field. The derivation of the series is for arbitrary values of k. By substituting the values of k appropriate for a conductor into the series the scattered fields appropriate for the conducting medium are found. The fields in the near vicinity of the sphere are then

plotted.

For large real values of k the series for the scattered fields has been noted to require many terms for convergence. For some situations the series results from cancellations of terms with very large magnitude. Asymptotic techniques can be used to approximate the series in these more difficult situations. For the evaluations performed in this paper with $|ka| = 20$ double precision evaluations were found to be largely untroubled by numerical errors.

Results -- Currents on the sphere

Previous evaluations of the fields near a sphere have undoubtedly been calculated, plotted and perhaps documented in the past, but the author is not familiar with many of them. The only plots known to the author are those of the current on the sphere itself due to King and Wu, (1957) as presented in Van Bladel (1964) (reproduced in Fig. 1 of this paper) functions related to the current calculated by Ducmanis and Liepa (1965) and presented in Bowman et al. (1969); and a plot of the electric field in Bowman et al. (1969) due to Huang and Kodis (1951). The results presented in these past papers are for real-valued wavenumbers.

For the sake of comparison with the results presented in Van Bladel (1964), the ϕ-component of the magnetic field on the $y = 0$ ($\phi = 0$) plane has been calculated at the surface of the sphere. The magnitude of this value, shown in Figure 2, corresponds to the magnitude of the theta component of the current shown in Fig. 1 (left-hand panel). The agreement is very good. (There is a slight discrepancy in the relative dependences at $k = 1.1$ and $k = 3.5$ near the 35° value of the abscissa. A check of the original King and Wu (1957) results leads to the conclusion that this discrepancy is probably due to the artist's rendering.) Note that in order to plot the results in the same format the abscissa of Fig. 2 is $180° - \theta$ where θ is the spherical polar angle defined in the previous section.

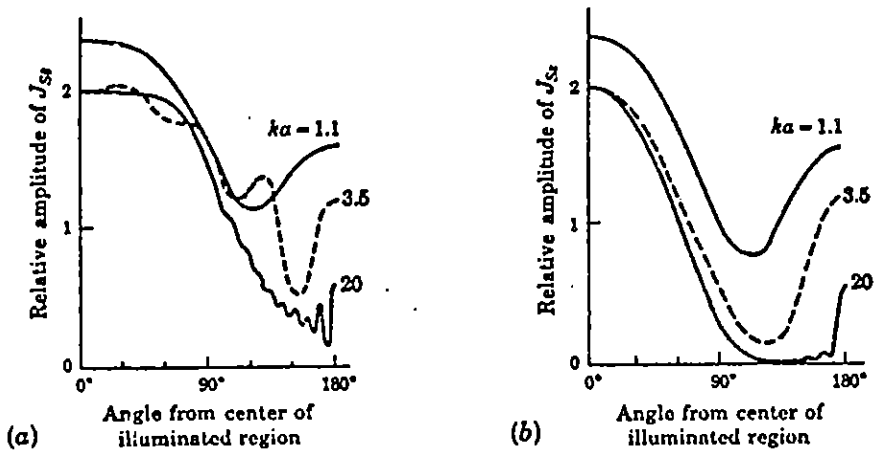

Figure 11.11 Current density at the surface of a sphere (*from R. W. P. King and T. T. Wu, "The Scattering and Diffraction of Waves," Harvard University Press, Cambridge, Mass., 1959, with permission of the President and Fellows of Harvard University*)

Figure 1. Current on the surface of a perfectly conducting sphere excited by an incident plane wave (from Van Bladel, 1964).

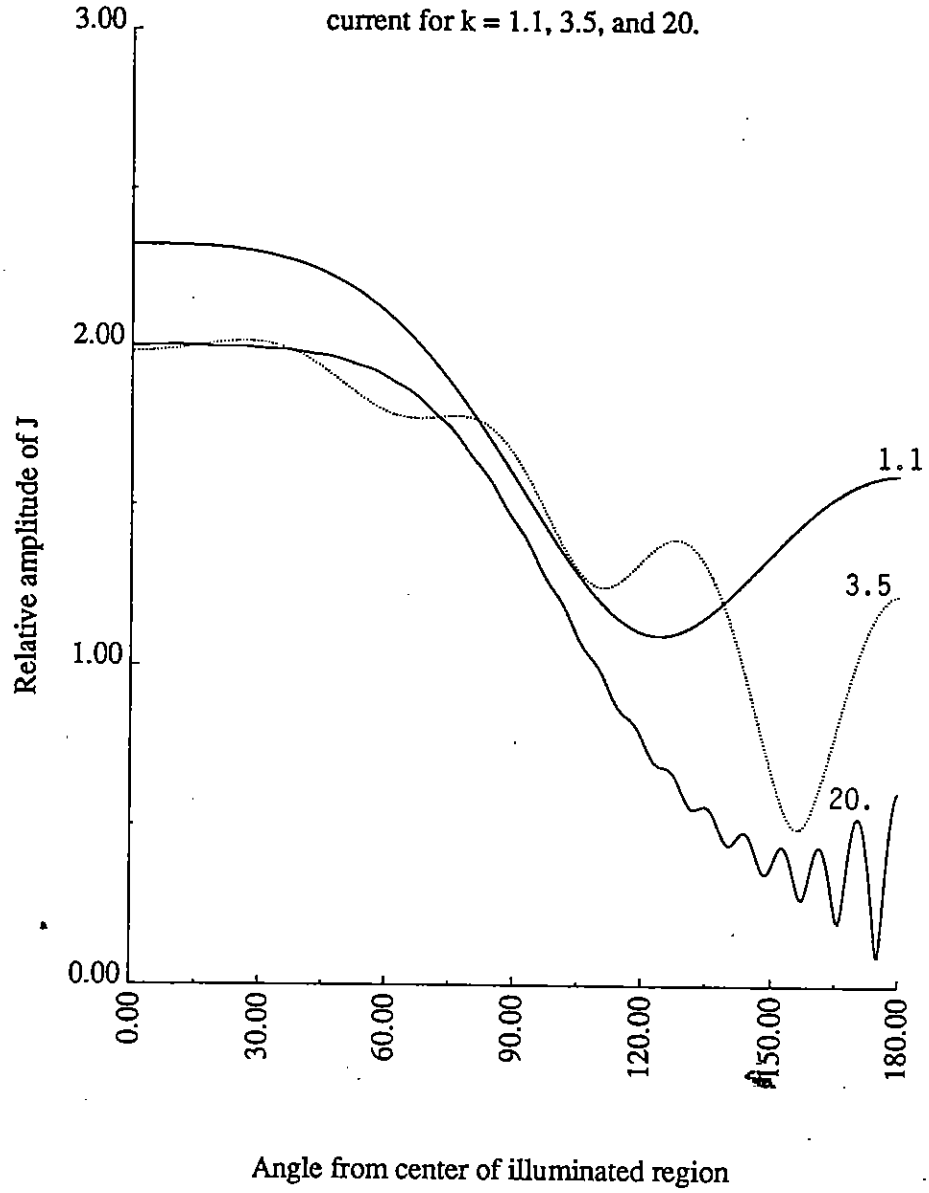

Figure 2. Calculated θ-component of the current on the surface of a perfectly conducting sphere for various real wavenumbers.

The development of a shadowed region as the wavenumber, k increases is apparent in Figures 1 and 2. For reference, at very small wavenumbers (say $k = .1$ or less) the current on the $\phi = 0$ plane has a magnitude of 1.5 independent of θ. As k increases, the current on the $y = 0$ plane increases on the illuminated side and decreases on the shadowed side. The current on the illuminated side approaches a value of 2 as k increases as is expected from geometric optics. The current on the shadowed side shows a trend to lower values as the wavenumber increases to 20. The geometric optics limit would be zero.

The current on the surface of the sphere has been calculated for wavenumbers with the same real values and with an imaginary value of -1.1 (Fig. 3). The imaginary component implies a lossy propagation of waves in the medium and for this choice of imaginary wavenumber component the waves are attenuated 2.2 e-folds in moving across a distance equal to the diameter of the sphere. To make meaningful comparisons and investigations into shadowing, the fields are normalized by the value of e^{-ikz}. For real-valued k this normalization only introduces a phase shift into the results which is not apparent in the amplitude plots. For values of k with a non-zero imaginary part this normalization effectively balances the expected exponential decay of the waves. This normalization has been applied for all plots presented in this paper.

From Fig. 3 it can be seen that the current in the shadowed region of the sphere in a lossy medium has local maximums of lower value than in pure dielectric. Evidently, the lossy nature of the media affects the interference properties of the creeping waves on the shadowed side of the sphere and the resulting peaks in the magnitude of the current are diminished. The average current nevertheless appears to be similar to that in Figs. 1 and 2.

In Fig. 4 results are shown with the imaginary part of the wavenumber set to -3.5. The real part is once again assigned values of 1.1, 3.5 and 20. The results found with the real parts of k equal to 3.5 or 20 are similar in average value to the results of Fig. 2 (no loss) and Fig. 3 (1.1 e-fold loss per unit distance). In this respect results with the

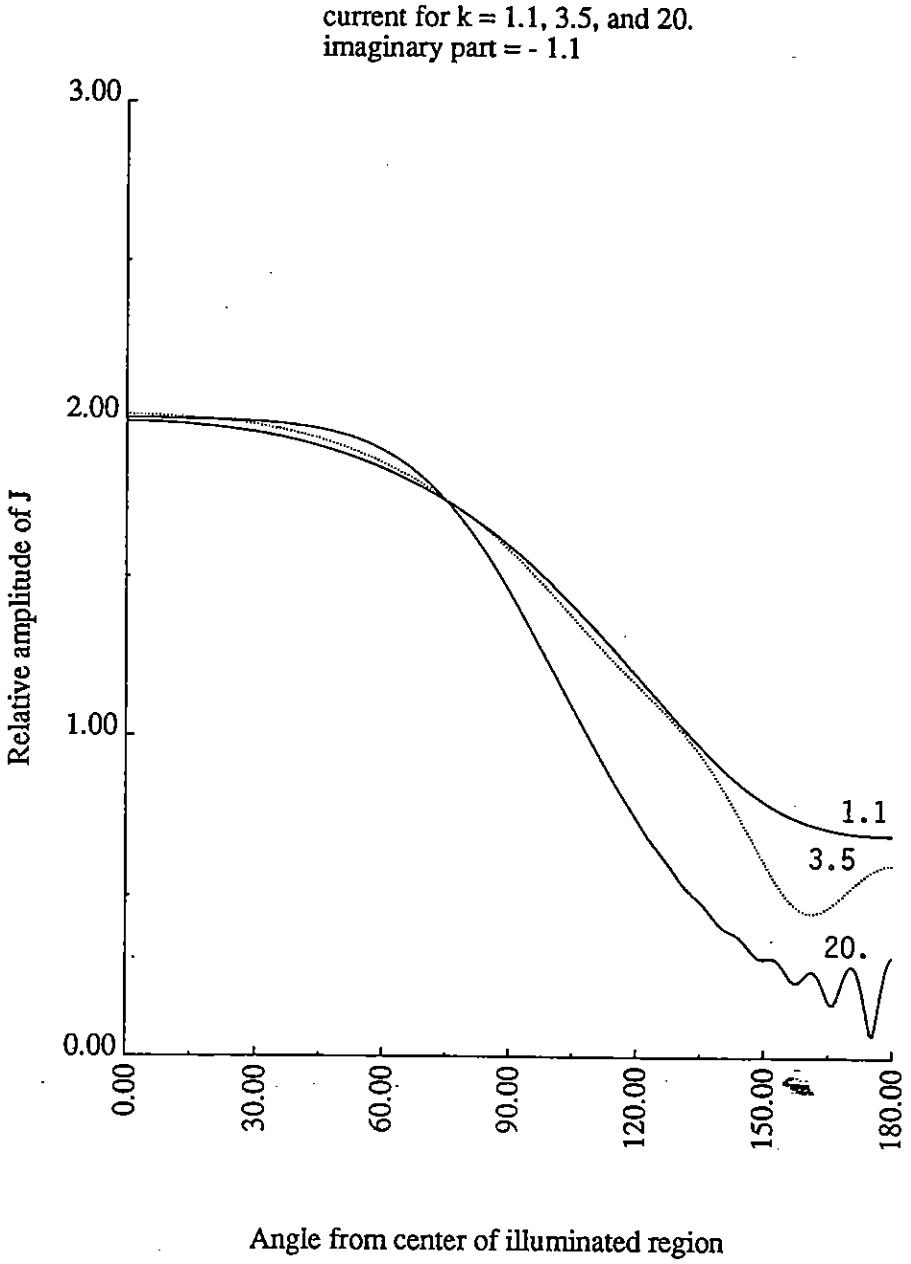

Figure 3. Calculated θ-component of current for various wavenumbers with imaging part set to -1.1.

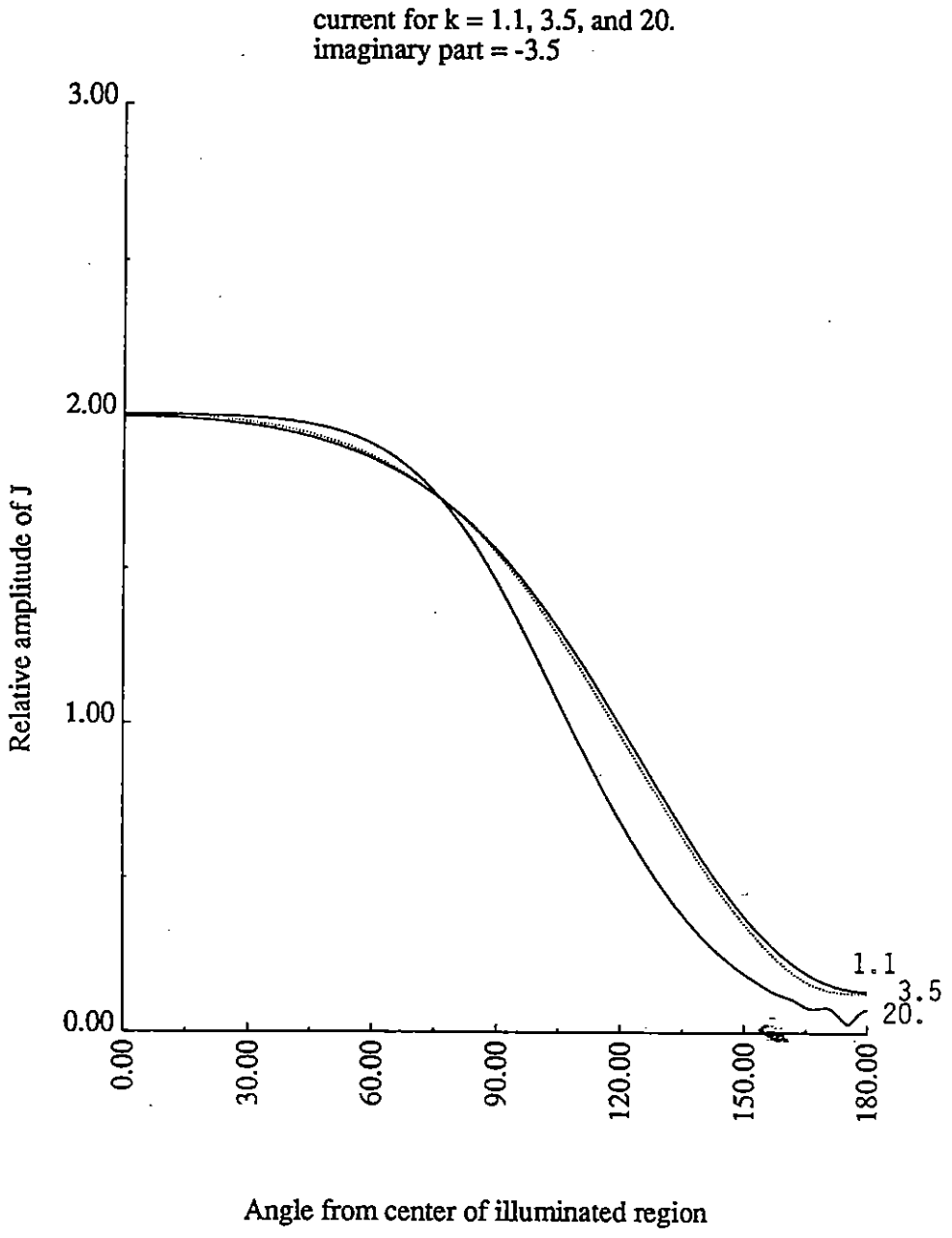

Figure 4. Calculated θ-component of current for various wavenumbers with imaginary part set to -3.5.

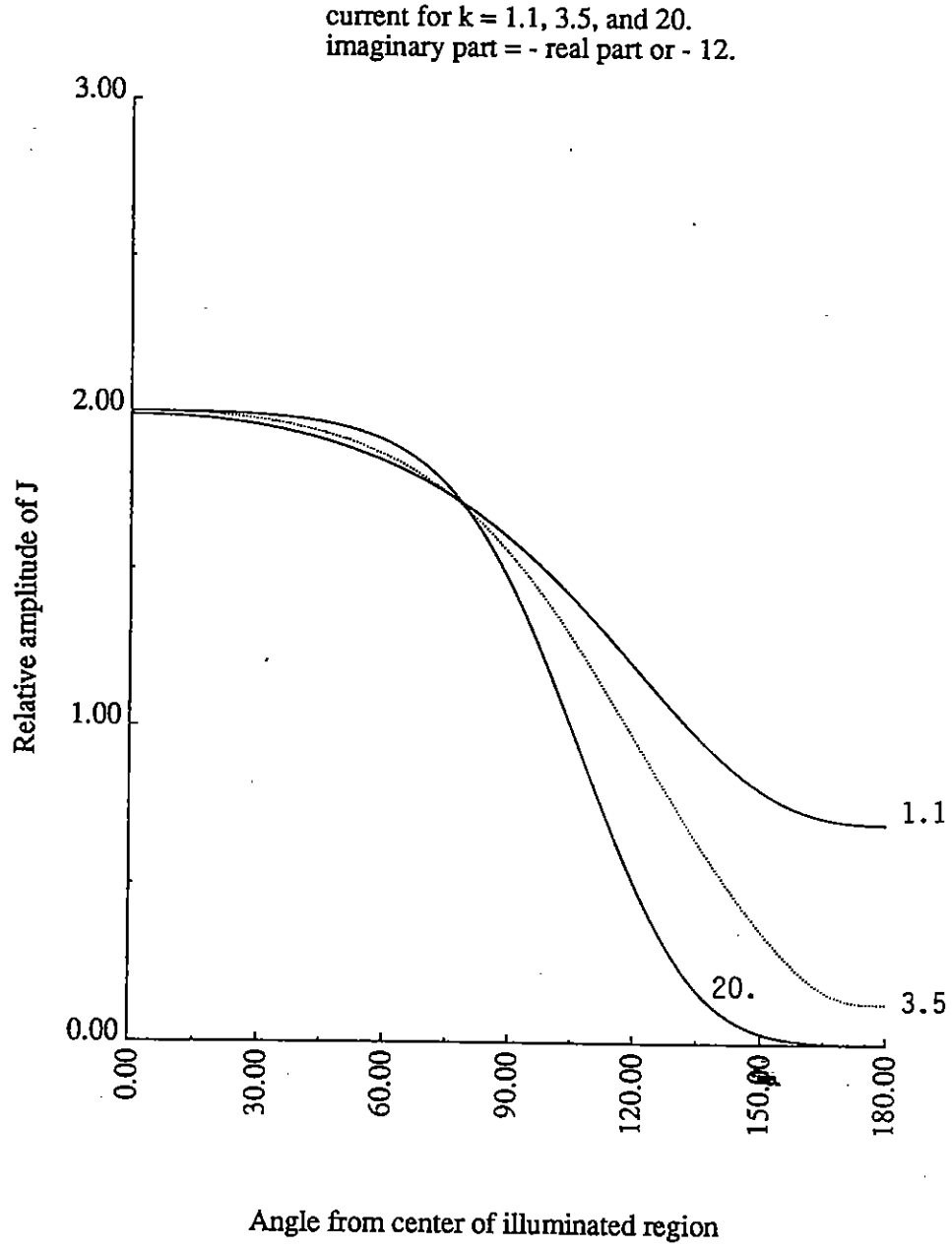

Figure 5. Calculated θ-component of the current for various skin depths.

real part of the wavenumber set to -1.1 differ in that they are not like those of Figs. 2 and 3. They are similar to the results with real part of the wavenumber set to -3.5 suggesting on a qualitative basis that it is the total magnitude of the wavenumber that controls the basic shadowing mechanism. The role of the imaginary component seems to primarily be the damping of creeping wave interference in the shadow zone.

Fig. 5 shows the current on the sphere for the cases $k = 1.1 - i1.1$, $k = 3.5 - i3.5$ and $k = 20 - i12$. The former two are for the case of spheres of various sizes in a good conductor and appear in Fig. 3 and 4 separately. It was initially desired to present the results for the wavenumber $k = 20 - 20i$, however, the results proved to be numerically ill-behaved. It is believed that the required normalization over 40 e-folds presents some difficulties even with 15 digit accuracy. As a substitute for this case the imaginary part is set to -12. It can be seen that the shadow region for this case becomes even more pronounced than it was in Fig. 2 thru 4. It is anticipated that at $k = 20 - i20$ the shadow would be qualitatively similar to that in Fig. 5.

The surface currents plotted in Figs. 1 thru 5 suggest that the shadowing properties of spheres embedded in conductors are similar to their shadowing properties in dielectrics. Small spheres don't shadow but large spheres do. The primary difference is that shadowing in conducting media is apparently deeper and smoother in spatial behavior than in dielectric media.

Results -- Near field of sphere

It is appropriate to investigate these properties further by the direct calculation of field patterns in the vicinity of the sphere. Accordingly, the field has been calculated for a range of real and complex wavenumbers on portions of two relevant planes. One plane, the $y = 0$ plane shows the general development of the shadow region as well as reflected waves. Figures 6 thru 9 show the amplitude and phase of the total E_x and H_y on this plane. The other plane lies behind the sphere at $z = 1.2$ (a distance of .2 from

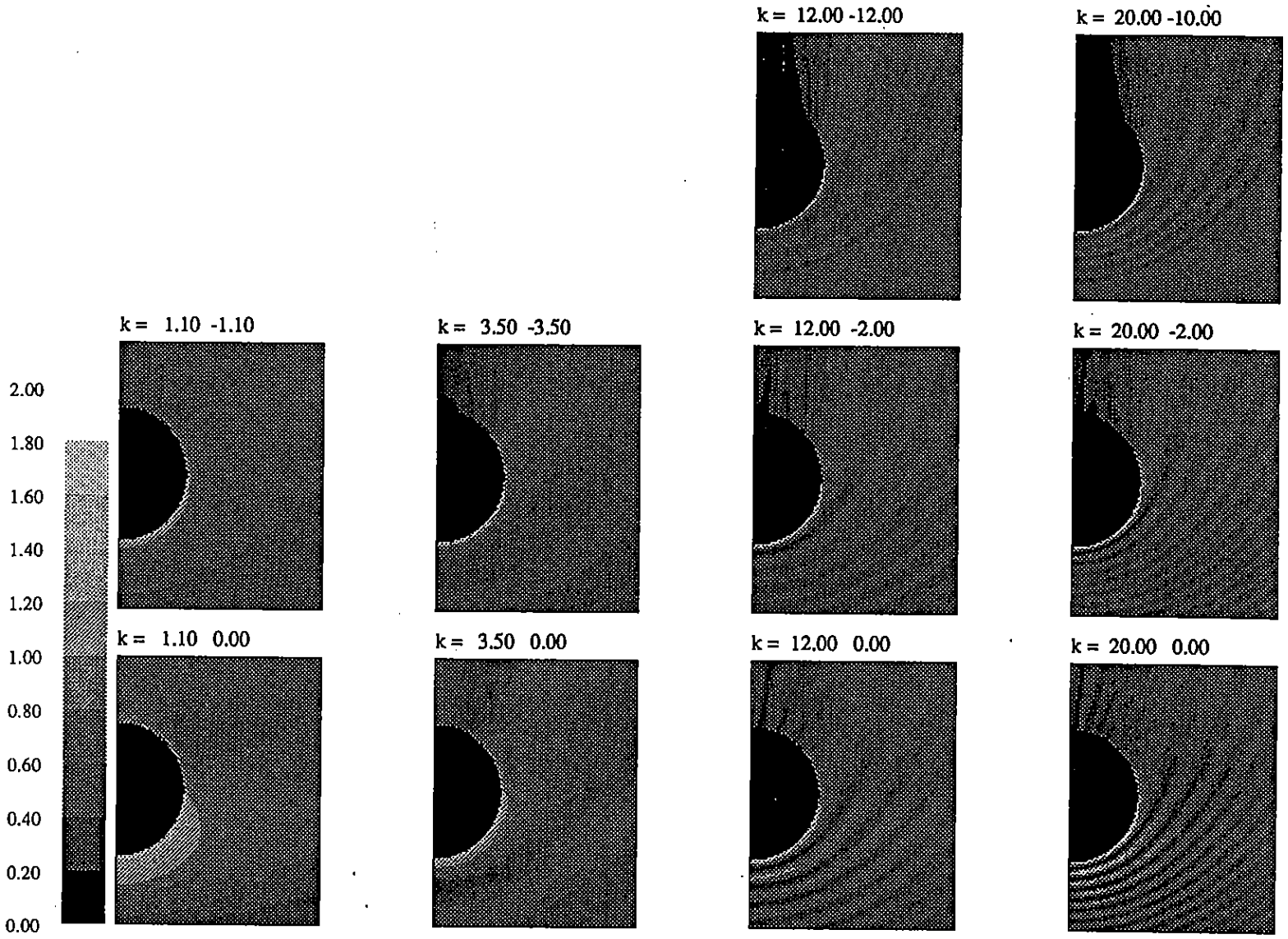

Figure 6. Magnitude of the y-component of the total magnetic field on the plane y = 0 .

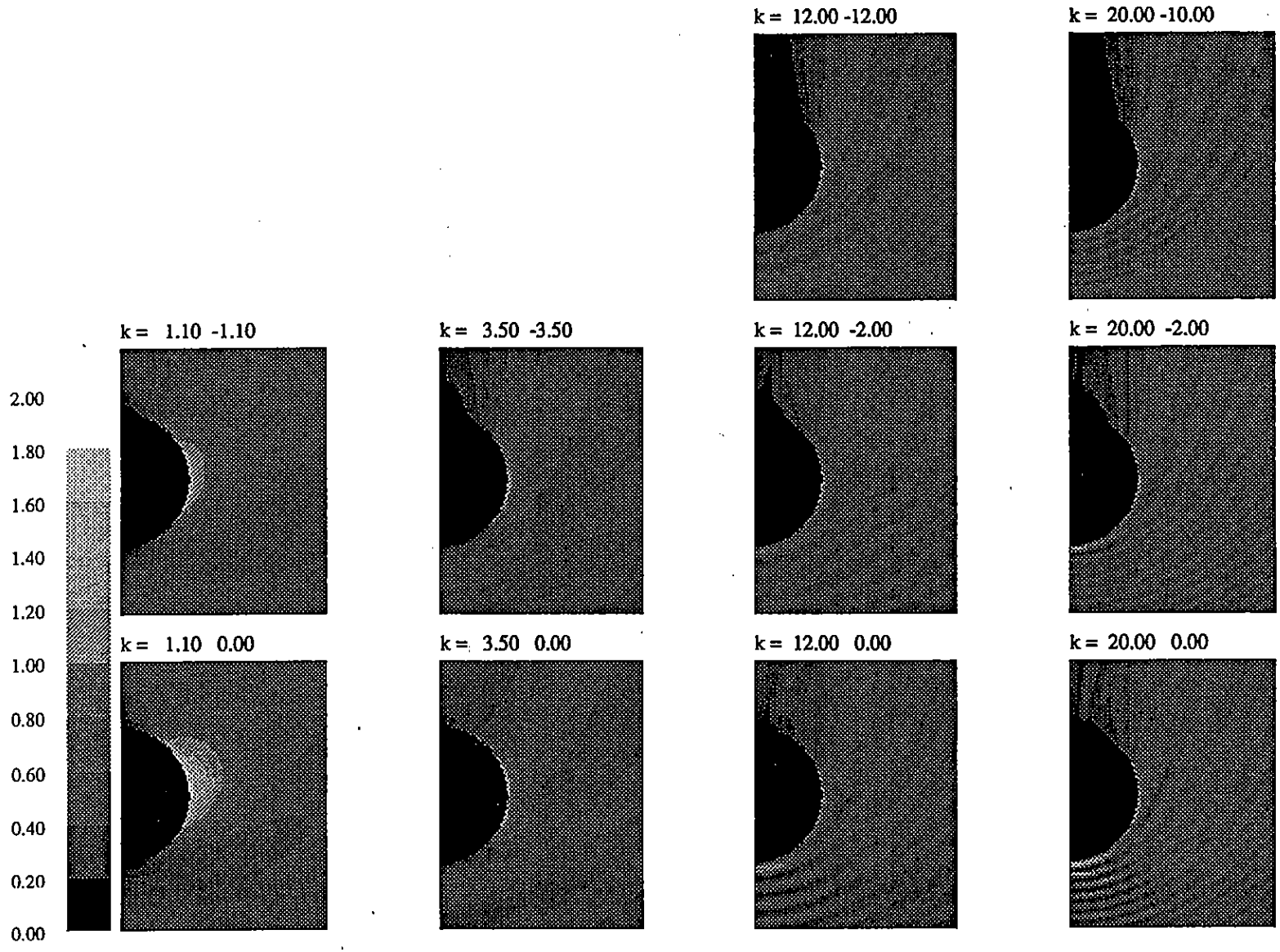

Figure 7. Magnitude of the x-component of the electric field on the plane $y = 0$.

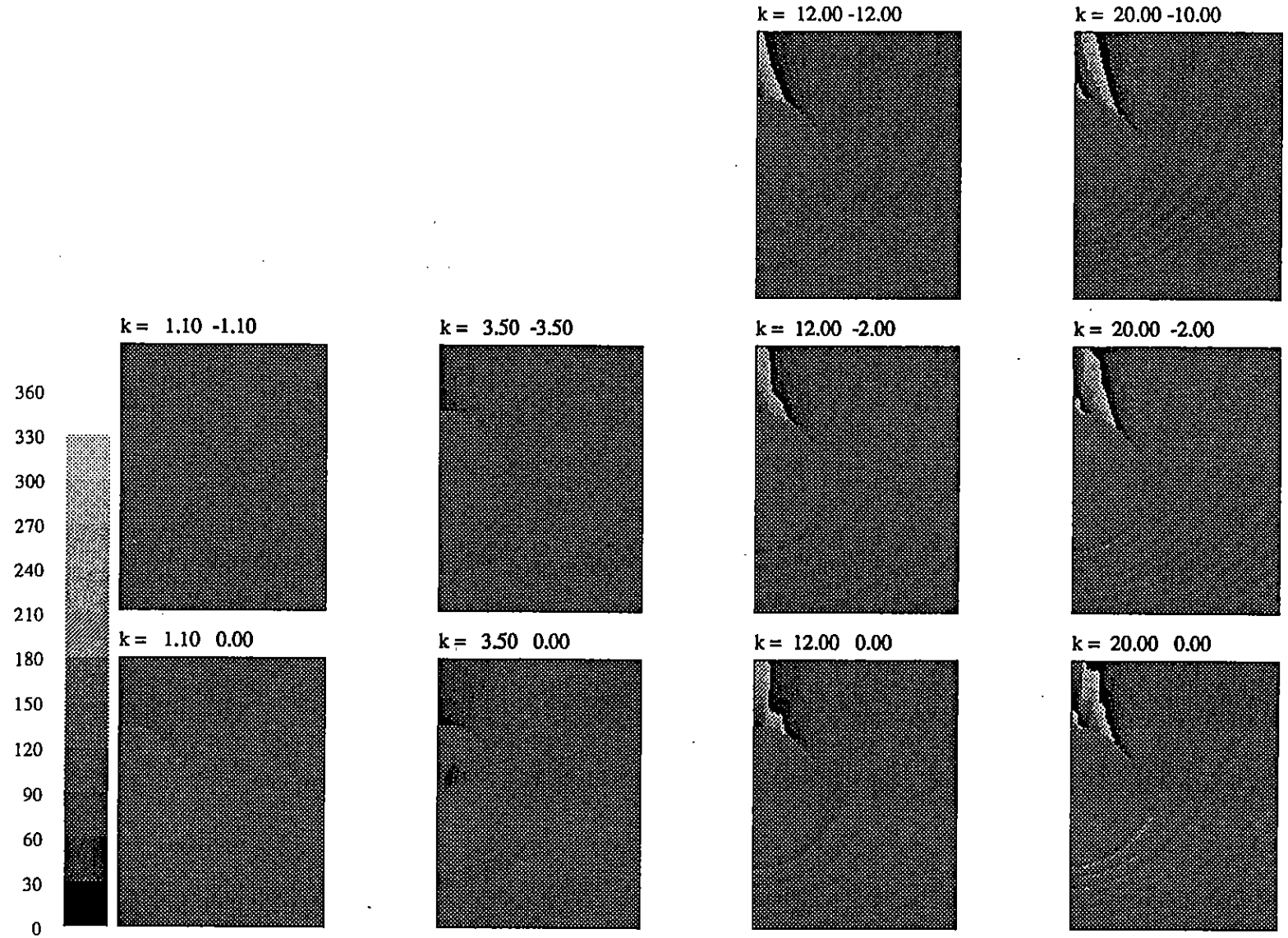

Figure 8. Phase of the y-component of the magnetic field on the plane $y = 0$.

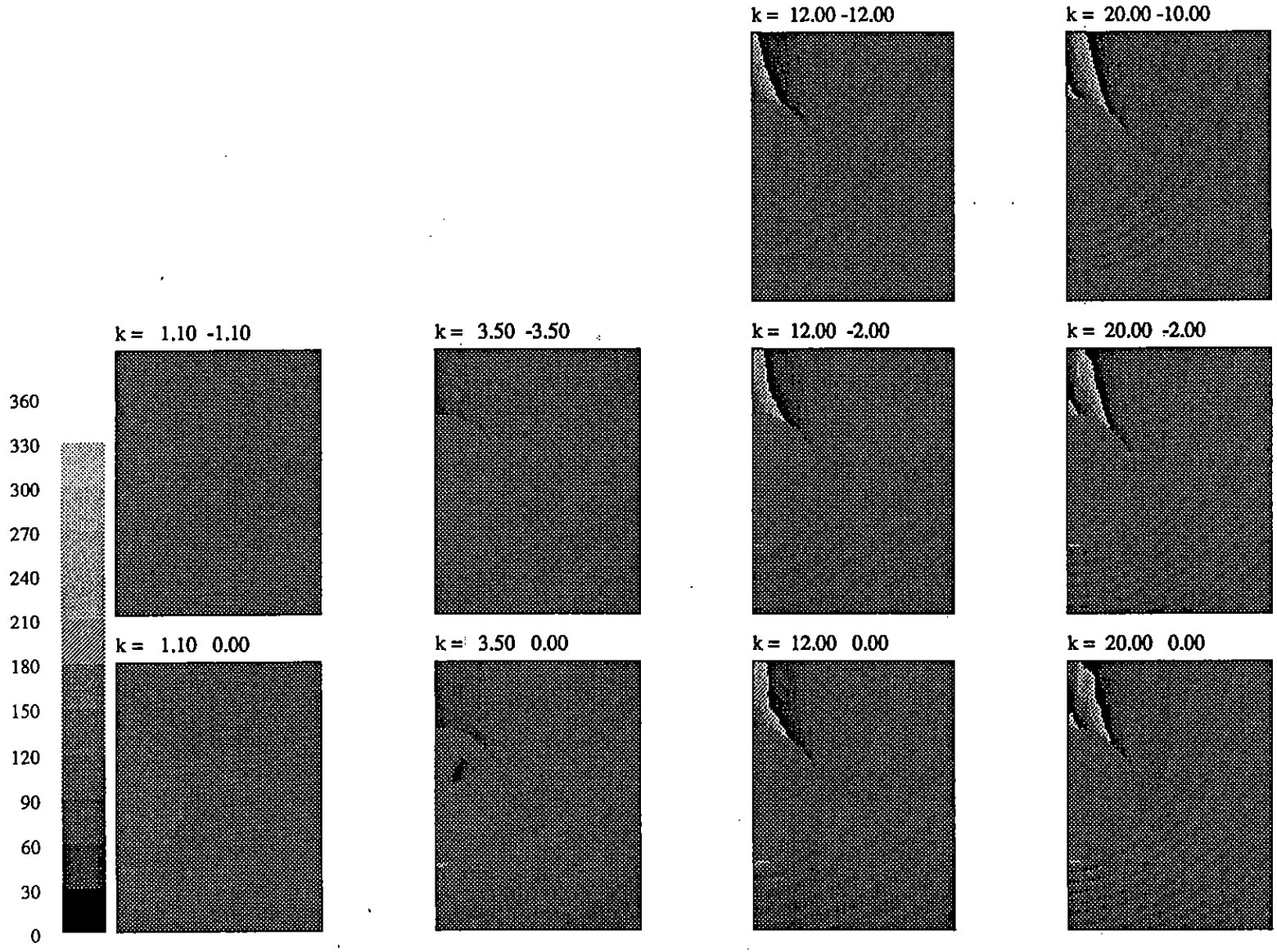

Figure 9. Phase of the x-component of the electirc field on the plane $y = 0$.

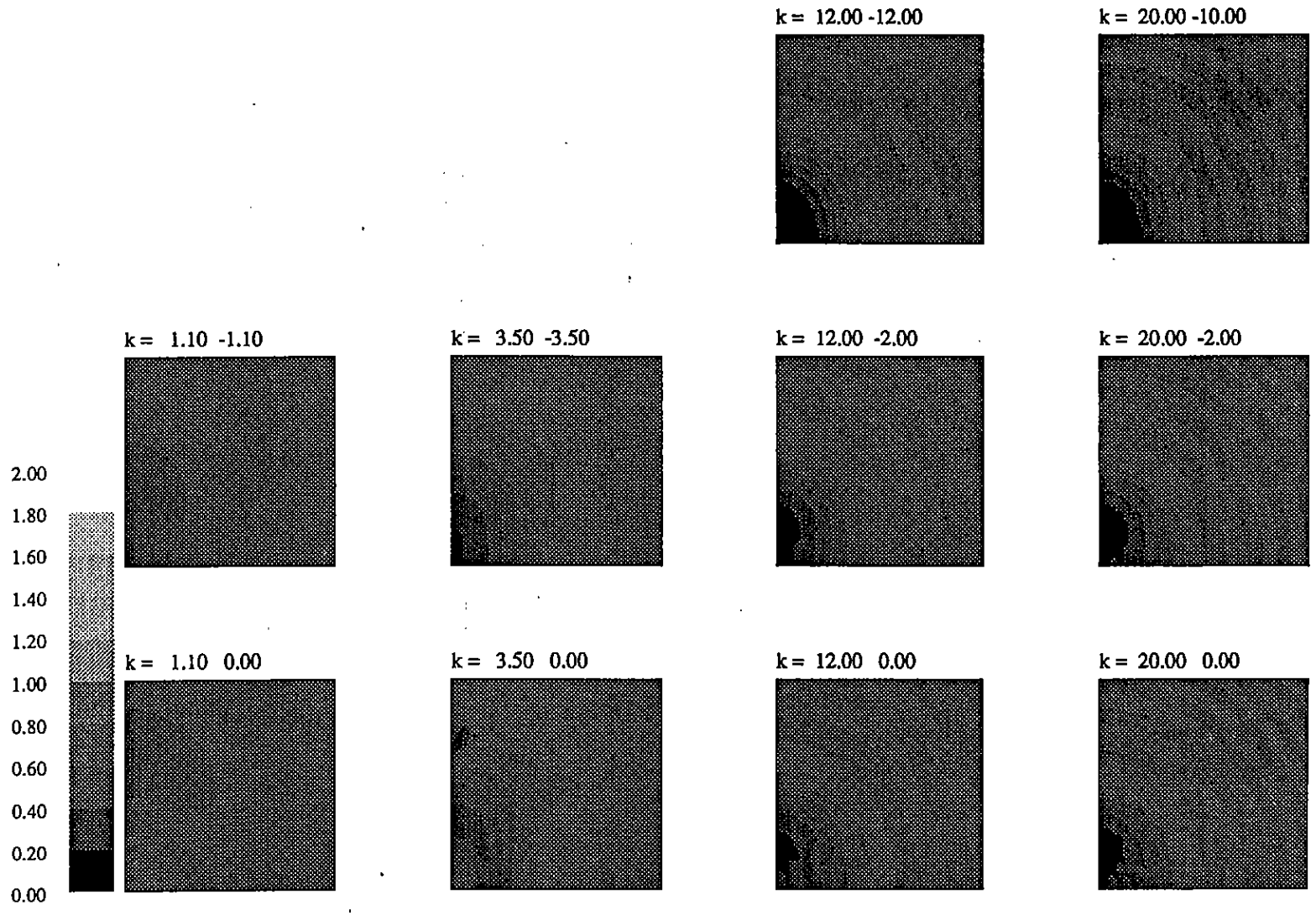

Figure 10. Magnitude of the y-component of the total magnetic field on the plane z = 1.2 a .

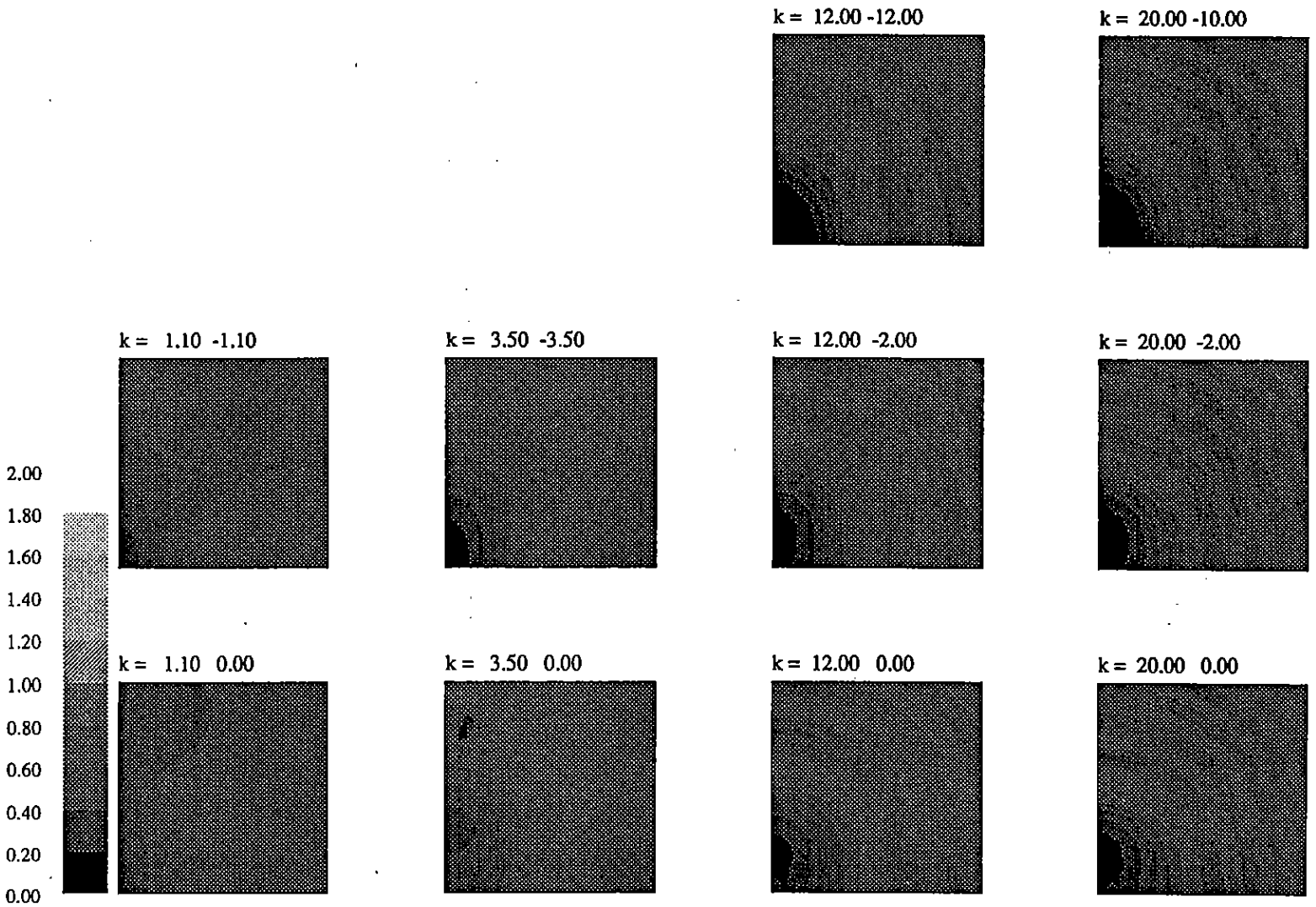

Figure 11. Magnitude of the x-component of the total electric field on the plane z = 1.2 a .

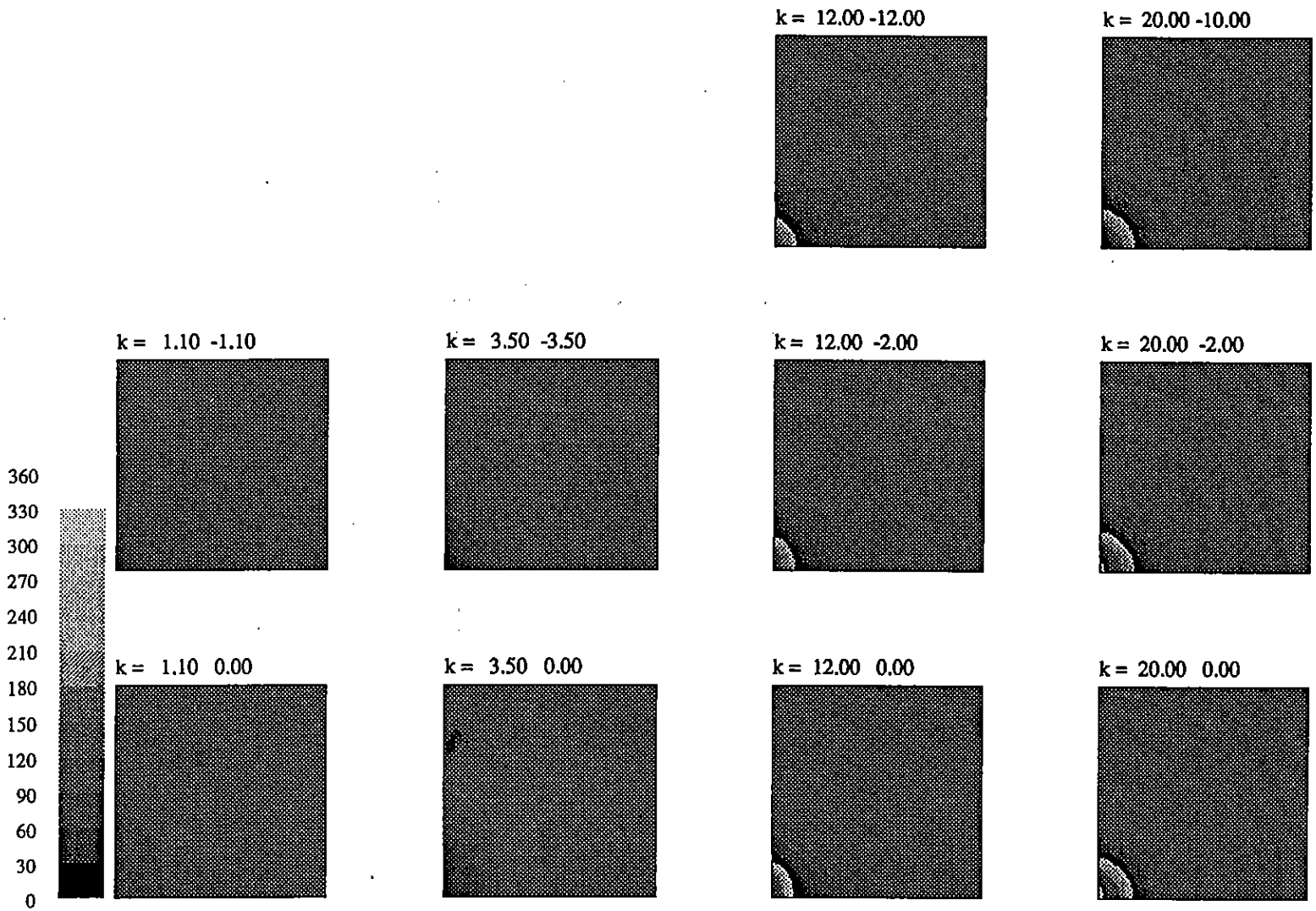

Figure 12. Phase of the y-component of the magnetic field on the plane z = 1.2 a .

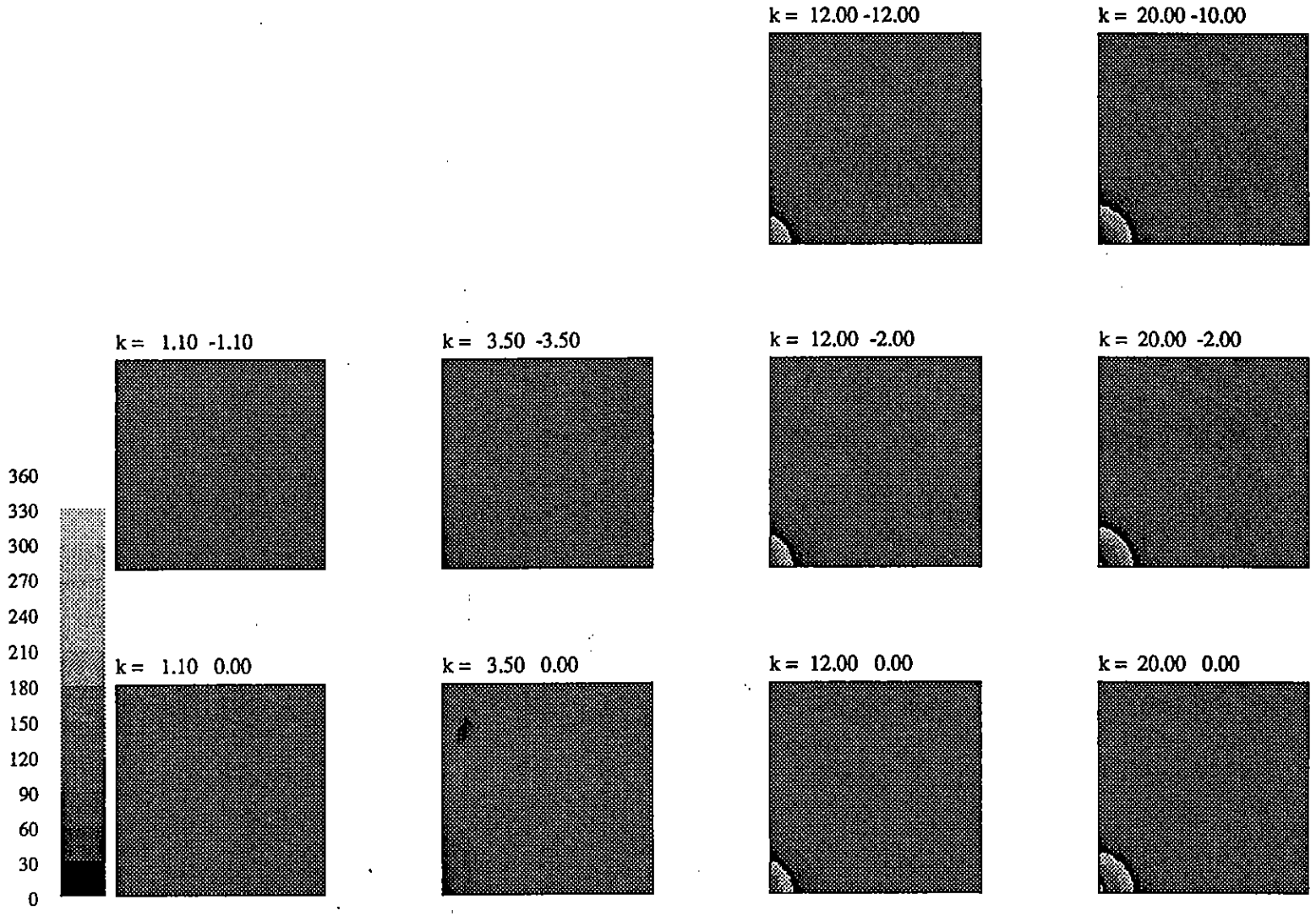

Figure 13. Phase of the x-component of the electric field on the plane z = 1.2 a .

the back of the sphere) and is perpendicular to the incident wave direction. (For convenience the distance units have been normalized by setting the spherical radius to 1 for all results.) Results from this plane reveal details of the shape of the near shadow region and whether any unexpected effects occur off the equatorial axis. Figs. 10 thru 13 show results from this plane. The results in these figures are discussed in further detail below but it is fair to note at this time that there are no surprises in them that change the conclusions already made about shadowing properties from the surface current values.

Fig. 6 shows 10 windows detailing results plotted with a gray-scale. Each window represents the results from a calculation at the wavenumber noted above it. The degree of shading in each window represents a magnitude according to the key shown in the lower left corner of the figure. Plotted in Figure 6 is the magnitude of the y-component of the total (incident plus scattered) magnetic field on the plane $y = 0$. For each figure the range of x is 0 to 3 shown from left to right and the range in z is -2 to +2 from bottom to top in each window. The y-component of the field is symmetric about the $x = 0$ plane. The dark semi-circular region in each square represents the interior of the perfectly conducting sphere where the field is zero. The calculations are performed on a 128 by 128 grid oriented in the $x - z$ direction. The granularity in the shape of the circle reflects the spatial resolution of the grid. The plane wave is incident from below. The interaction of the reflected wave and the incident wave is especially apparent in the lower portions of the $k = 3.5$, $k = 12$ and $k = 20$ windows and to some degree in the $k = 12 - 2i$ and $k = 20 - 2i$ windows. The values plotted in each of the windows have been normalized so that the incident wave has a value of 1 everywhere even for the lossy media. The geometric optics value of 2 is attained on the illuminated side of the sphere in all the windows. Shadowing is evident in the windows with the results from the higher-valued wavenumbers displayed.

A similar trend is seen in the plot of magnitude of the x-component of the total electric field seen in Fig. 7. The format of Figure 7 is the same as Figure 6. The electric

field is unlike the magnetic field in that the total x-component goes to zero near $x = 0$ $z = \pm 1$. Despite the different boundary condition the shadowing behavior of the field is much the same as that in Fig. 6.

Figures 8 and 9 respectively show the phase of the total magnetic y and electric x field components. To avoid extensive regions where the phase might shift from 0 to 360 the values have been biased by 180°. Thus the normalization for these plots makes the phase of the incident wave 180° everywhere. Evident in both Figures 8 and 9 is the phase retardation as the creeping waves circle the sphere in the shadow zone. This same phenomena occurs in the shadow zone of both dielectric and conducting media.

Figures 10 thru 13 shows the results of calculations on the $z = 1.2$ plane for the same wavenumbers as shown in Figures 6 thru 9. Each window in each of the figures represent the results of calculations made on a 128 by 128 grid oriented in the x–y direction. For Figures 10 thru 13 the range in x is 0 to 3 from left to right and the range in y is 0 to 3 from bottom to top. The results are symmetric about the x- and y-axes on the bottom and left-hand edges of each window.

The magnitudes of the magnetic field (Fig. 10) and the electric field (Fig. 11), show the same tendency between shadowing and wavenumber as seen in previous results. Higher wavenumber media have shadows whereas lower wavenumber media do not. Lossy media have shadows that are more pronounced and smoother than non-lossy media. The results show that the shadows tend to be darker along the $x = 0$ line than along the $y = 0$ line, especially for the less lossy wavenumbers. For the more lossy results the shadow profile appears to be more uniform.

The phase of the field is also similar to that seen in Figs. 8 and 9 in that the phase retards as one enters the shadow zone. Not surprisingly, higher wavenumbers have larger phase retardation in their shadows. It may be a bit surprising, however, that the contours of constant phase are somewhat elliptical and elongated in the y-direction for the smaller wavenumbers. This elongation is symptomatic of the sensitivity of the scattering process to the polarization of the incident wave.

Conclusions

The Mie series for the field scattered by a perfectly conducting sphere has been evaluated and plotted for complex values of wavenumber in order to explore the near-field shadowing properties of objects in a lossy dielectric or in a conducting medium. Near field shadows appear to be controlled by the product of the magnitude of the wavenumber of the medium and the structure size. Apparently, the 90° phase shift between the (displacement) current in the medium and the electric field, a relation that characterizes dielectric media, is not a necessary requirement for the shadowing process to occur in an arbitrary medium. The shadows produced in a lossy dielectric were spatially smoother than those produced in dielectric with the same magnitude wavenumber. For conducting media with skin depths smaller than the radius of the sphere by a factor of three or more, shadows were produced.

References

Baum, C.E., "On the singularity expansion method for the solution of electromagnetic interaction problems," Interaction Notes, Note 88, December, 1971.

Bowman, J.J., T.B.A. Senior, P.L.E. Uslenghi (editors), Electromagnetic and Acoustic Scattering by Simple Shapes, New York, Hemisphere Publishing Corporation, 1969 (Revised printing, 1987).

Ducmanis, J.A. and V. V. Liepa, "Surface field components for a perfectly conducting sphere," The University of Michigan Radiation Laboratory Report No. 5548-3-T, Ann Arbor, Michigan (1965).

Harrington, R.F., Time Harmonic Electromagnetic Fields, New York, McGraw-Hill Book Company, 1961.

Huang, C. and R.D. Kodis, "Diffraction by spheres and edges at 1.2 cm," Harvard University Craft Laboratory Technical Report No. 138, Cambridge, Massachusetts (1951).

Jackson, John David, Classical Electrodynamics, New York, John Wiley & Sons, 1962.

Jones, D.S., The Theory of Electromagnetism, Oxford, Pergamon Press, 1964.

King, R.W.P. and T.T. Wu, The Scattering and Diffraction of Waves, Cambridge, Mass., Harvard University Press, 1959.

Panofsky, Wolfgang K.H. and Melba Phillips, Classical Electricity and Magnetism, Reading, Massachusetts, Addison-Wesley Publishing Company, Inc., second edition (1962).

Stratton, Julius Adams, Electromagnetic Theory, New York, McGraw-Hill Book Company, 1941.

Van Bladel, J., Electromagnetic Fields, New York, McGraw-Hill Book Company, 1964.